

Study on the Temporal Evolution of Literature Bradford Curves in the Context of Library Specialization

Haobai Xue¹, Xian Liu^{2*}

(1. xuehb@utszlib.edu.cn; Shenzhen Science & Technology Library/University Town Library of Shenzhen, 2239 Lishui Road, Nanshan District, Shenzhen 518055, China;

2. xliu@shenzhong.net; Shenzhen Middle School, 1068 Nigang West Road, Luohu District, Shenzhen, Shenzhen 518055, China)

Abstract:

The Bradford's law of bibliographic scattering is a fundamental law in bibliometrics and can provide valuable guidance to academic libraries in literature search and procurement. However, the Bradford's curves can take various shapes at different time points and there is still a lack of causal explanation for it, so the prediction of its shape is still an open question. This paper attributes the deviation of Bradford curve from the theoretical J-shape to the integer constraints of the journal number and article number, and extends the Leimkuhler and Egghe's formula to cover the core region of very productive journals, where the theoretical journal number of which fall below one, $f_t(X_i) = C/X_i^\alpha < 0$. The key parameters of the extended formula are identified and studied by using the Simon-Yule model. The reasons for the Groos Droop are explained and the critical point for the shape change are studied. Finally, the proposed formulae are validated with the empirical data found in the literature. It is found that the proposed method can be used to predict the evolution of Bradford's curves and thus guide the academic library for scientific literature procurement and utilization.

Key words: Simon-Yule model, Bradford, dynamics, extreme statistics

1 Introduction

1.1 Introduction

As one of the three fundamental laws of bibliometrics, the Bradford's law of bibliographic scattering has many potential applications in academic libraries. For example, it can be used to determine the core journals or publishers of a certain research area and thus provides guidance to the librarians for the procurement of journals and books (Barrantes, Dalton et al. 2023). Besides, it can also be used to quickly locate the key WoS research areas or IPC classes for a topic and thus provides assistance for the readers/librarians in the literature search (Sheikh, Zahra et al. 2022). However, the preparation of the Bradford's curves takes time, especially for the trivial many journals with only one or two relevant papers. Worse still, the scientific literature of a certain discipline or research area usually increases exponentially or undergoes different developmental stages (Larivière, Archambault et al. 2008), so strictly speaking the Bradford's curve prepared at any time point cannot be used directly many years later without adjustment. There are some mathematical formulae that can help predict the shape of Bradford's curve, but they usually result in a J-shaped curve while in practice, the Bradford's curve can take at least six different shapes, with the most notable being the S-shaped curve with the so-called Groos Droop (Groos 1967). It is suggested that there is a lack of causal explanation of this bibliometric law and a lack of comprehensive empirical examples (Wagner-Döbler 1997). Therefore, the prediction of the evolution of Bradford's curve is still an open

question and merit further investigation.

This paper tries to attribute the different shapes of Bradford's curve to the integer constraints of journal number and paper number. If the journal productivity n goes so high that the corresponding theoretical journal number $f_t(n) = C/n^\alpha$ falls below one, then the actual journal number can only choose between zero and one. As a result, the discrete nature of journal number causes the core zone to deviate from the theoretical results of Lotka or Simon-Yule model. To remedy this problem, this paper proposes two different formulae for the core zone and the trivial-many zone respectively, and key parameters of the formulae are identified and studied through theoretical analysis and Monte Carlo simulation of the Simon-Yule model. The reasons for the Groos Droop are explained and the critical point for the shape change are studied. Finally, the proposed formulae are validated with the empirical data found in the literature. It is found that the proposed method can be used to predict the evolution of Bradford's curves and thus guide the academic library for scientific literature procurement and utilization.

1.2 Literature Review

The Bradford's law was first proposed by Bradford in 1934 (Bradford 1934) but did not receive wide recognition until Vickery further develop this theory in 1948 (Vickery 1948). According to Bradford's law, if we arrange journals in descending orders of their productivity and divide them into p groups with the same number of papers, then the number of journals in each group n_i follows $n_1:n_2:\dots:n_p = 1:k:\dots:k^{p-1}$, where k is a constant referred to as the Bradford multiplier. In addition to the above-mentioned verbal form, the Bradford's law can also be shown as a J-shaped Bradford curve by plotting the accumulated productivity $R(r)$ of the first r journals against the natural log of the journal rank r . The mathematical formula of Bradford's curve was proposed by Leimkuhler in 1967 (Leimkuhler 1967) and the method for determining the parameters of this formula was published by Egghe in 1990 (Egghe 1990). In Egghe's formula, $R(r) = a \log(1 + br)$, where the key parameters a and b can be calculated from the article number A , journal number T , and the productivity y_m of the most productive journal. Although the Egghe's formula matches well with many bibliographies, it corresponds to a J-shaped Bradford's curve which will inevitably deviate from those bibliographies with a Groos Droop (Egghe 1990). Incomplete bibliography is first believed to be the reason of the Groos Droop, but further research refuted this hypothesis (Qiu and Tague 1990) and it has been proved by Egghe that if the ranking of each journal r is transformed into $r' = r + r_0$ by adding a large constant $r_0 > 1/b$, then the new curve will concave downwards and thus show a Groos Droop (Egghe and Rousseau 1988). The merging of different bibliographies (each with a different maximum journal productivity $y_m^{(i)}$) could be one possible reason for the large constant r_0 (Egghe and Rousseau 1988), but it is also likely that the large core regions (regions of most productive journals with theoretical journal number $f_t(n_i) < 1$) of some bibliographies result in the large r_0 (Chen and Leimkuhler 1987). Essentially, the y_m in Egghe's formula denotes the journal productivity which satisfies $f_t(y_m) = C/y_m^\alpha \approx 1$ (Egghe 1985), rather than the maximum yield X_1 of a journal as claimed by Egghe himself. Therefore, there might be a core region of significant few journals, each with a theoretical journal number $f_t(X_i) = C/X_i^\alpha < 1$ ($i = 1, 2, \dots, T_0$), and if the total number of these journals T_0 exceeds the critical value $r_0 = 1/b$, then a Groos Droop will emerge. In this paper, the latter explanation is adopted and the Egghe's formula is extended accordingly to predict the evolution of Bradford's curves.

In the 1990s, the research interest on the Bradford law has gradually shifted from the static presentation of data at a particular time point toward the time-dependent, dynamic and evolutionary aspects (Oluić-Vuković 1998). Oluić-Vuković studied how the increase in productivity of core journals affected the shape of the distribution curve in the upper section over an extended time interval (Oluić-Vuković 1989). By analyzing the research output of Croatian scholars in different subjects, she concluded that the Groos Droop or the S-shaped curve is caused by increase in the concentration/dispersal disparity, which can be reflected by the increase in the core/periphery ratio (Oluić-Vuković 1991). The dynamic evolution of Bradford curves and the emergence of Groos Droop are presented in (Oluić-Vuković 1992), and other similar empirical studies through the temporal partitioning of bibliographies are conducted by Garg (Garg, Sharma et al. 1993), Wagner-Döbler (Wagner-Döbler 1997) and Sen (Sen and Chatterjee 1998). Meanwhile, stochastic models such as the Simon-Yule model have been increasingly employed to study the dynamic characteristics of bibliometric laws (Oluić-Vuković 1997, Oluić-Vuković 1998). The Simon-Yule model is initially introduced by Yule in 1924 for studying the distribution of biologic genera distribution by species number, but does not gain widespread recognition until Simon expanded upon this theory in 1955 to analyze the frequency distributions of words in writing samples (Simon 1955). In addition to employing theoretical methods for precisely solving the constant entry rate α of new sources (Simon 1955), Monte Carlo simulations are utilized to explore more intricate scenarios, such as the declining entry rate α_t of new sources (Simon and Van Wormer 1963) and the autocorrelated growth rate γ of established journals (also referred to as the aging or obsolescence of older journals) (Ijiri and Simon 1977). Chen et al. (Chen 1989, Chen, Chong et al. 1994, Chen, Chong et al. 1995) first employed the Simon-Yule model for numerically studying the evolution of Lotka's law and Bradford's law over time. They found the entry rate of new sources α_t and the autocorrelated growth rate of old journals γ have significant yet opposite effect on the Bradford curves and thus offered an explanation for the various types of Bradford curves (Chen, Chong et al. 1995). Later, Oluić-Vuković also delved into the dynamics of Bradford distribution using the Simon-Yule model, but she found that the steady-state solution of this model is too restricted to cope with the variation produced in time, thereby limiting its applicability (Oluić-Vuković 1997, Oluić-Vuković 1998). In this paper, the Simon-Yule model is also utilized to examine the effects of different scenarios on the key parameters (e.g., journal number T_0 , article number A_0 and maximum productivity X_1 of the core region) of the extended Egghe's formula. However, it is not directly employed to forecast the evolution of Bradford curves or to compare them with empirical data. Instead, the key parameters are estimated from past empirical data to enhance predictions of Bradford curve evolution in the future.

2 Theoretical Study

2.1 Simon-Yule Model

The Simon's generating mechanism for the Bradford distribution is based on the following two assumptions, where the $f_t(n, k)$ denotes the number of journals that have published exactly n papers in the first k published papers.

Assumption I: There is a constant probability α that the $(k + 1)$ -th paper is published in a new journal – a journal that has not published in the first k papers;

Assumption II: The probability that the $(k + 1)$ -th paper is published in a journal that has

published n papers is proportional to $nf(n, t)$ – that is, to the total numbers of papers of all journals that have published exactly n papers.

Therefore, if there are A papers at a certain time point, then the corresponding journal number T is approximately $T = A\alpha$. Based on Simon's two assumptions, the steady-state solution of the Bradford distribution can be written as (Chen 1989):

$$f_t(n) = \rho B(n, \rho + 1) \approx \rho \Gamma(\rho + 1) n^{-(\rho+1)} \quad (1)$$

where B is the beta function, Γ is the gamma function, and ρ is a function of the entry rate of new source α , $\rho = 1/(1 - \alpha)$. From equation (1) it can be noted that the analytical result of the Simon-Yule model is in accord with the Lotka's law as long as $\rho \approx 1$.

In addition to the analytical solutions, Monte Carlo simulations are carried out for the case $\alpha = 0.1$, and the results are compared with the theoretical results of equation (1), as shown by Figure 1. The procedures for conducting the Monte Carlo simulations can be found in Reference (Simon and Van Wormer 1963) and thus omitted here. In order to minimize the randomness inherent in this stochastic model and more accurately capture the underlying rule, each case is simulated $N = 10000$ times, and only the means of all these simulations are used as the final outputs.

From Figure 1, it can be clearly noted that the simulation results can be divided into two zones, namely the normal zone (blue circles) and the core zone (red squares). This division is due to the fact that the actual journal number $f_e(n)$ must be integers and cannot fall below one, so when the journal productivity n is so large that the corresponding theoretical journal number $f_t(n)$ fall below one, then the actual journal number $f_e(n)$ will forcibly choose between zero and one, thereby deviating from the theoretical results, as shown by the red squares in Figure 1. Meanwhile, it can be noted from Figure 1(b) that although the number of journals of the core region is small, its contribution to the number of papers is significant. Therefore, it will be crucial to predict the corresponding paper number of each journal X_r in the core zone in order to depict the Bradford's curve accurately.

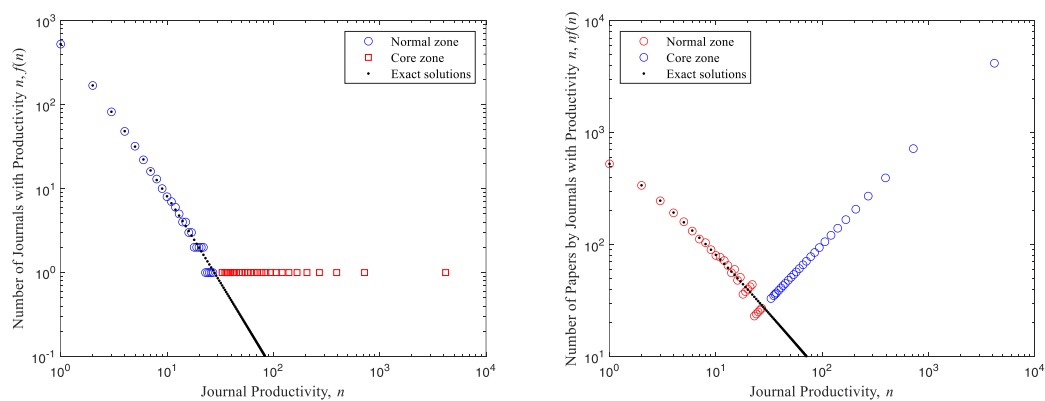


Figure 1 Comparisons of the theoretical and numerical results: (a) number of journals $f(n)$ with productivity n ; (b) number of papers $nf(n)$ by journals with productivity n

In order to estimate the journal productivity X_r of the core region, it will be helpful to figure out the journal number T_0 and paper number A_0 first. From Figure 1 it can be noted that the journal number $f(n)$ and paper number $nf(n)$ of the normal region matches very well with the

theoretical results, so the total journal number T_1 and total paper number A_1 of the normal region can be directly obtained by summing up all the journal and paper number, $T_1 = \sum_{n=1}^{y_m} f(n)$, and $A_1 = \sum_{n=1}^{y_m} nf(n)$, where y_m is the journal productivity when $f(y_m) \approx 1$. According to Equation (1), the analytical expression of the y_m can be derived as:

$$y_m = [A(\rho - 1)\Gamma(\rho + 1)]^{\frac{1}{\rho+1}} \quad (2)$$

After y_m is calculated, then the total number of journals T_0 and papers A_0 of the core region can be calculated by $T_0 = T - T_1$ and $A_0 = A - A_1$. Or, the total number of journals T_0 and papers A_0 can be directly calculated by:

$$T_0 \approx \int_{y_m}^{+\infty} Tf(n) dn = \frac{y_m}{\rho} \quad (3)$$

$$A_0 \approx \int_{y_m}^{+\infty} Tnf(n) dn = \frac{y_m^2}{\rho - 1} \quad (4)$$

where y_m is calculated by Equation (2).

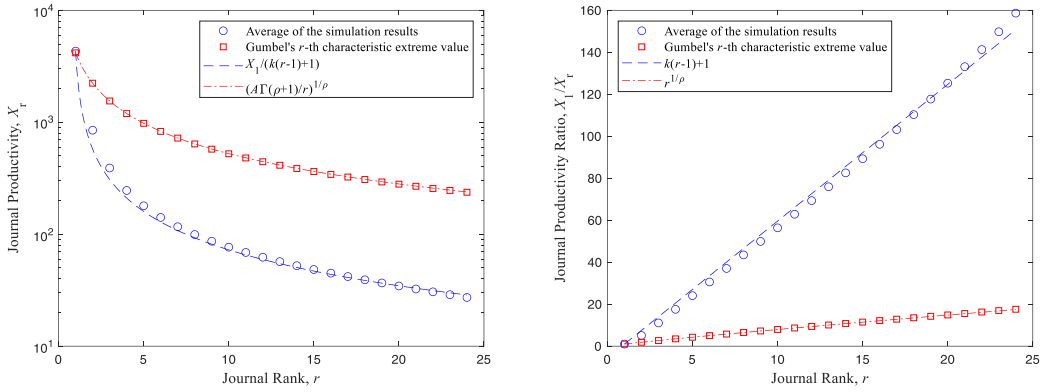


Figure 2 the journal productivity of the core region as functions of the journal rank: (a) the journal productivity X_r ; (b) the journal productivity ratio X_1/X_r

In the Simon-Yule model with constant entry rate α , It is found that the largest paper number one journal can have X_1 can be estimated by using the Gumbel's r -th characteristic extreme theory (Glänzel 2010, Glänzel 2013), which is:

$$G(X_r) \approx \int_{X_r}^{+\infty} f(i)di = \frac{r}{A} \quad (5)$$

By solving this equation, it can be derived that the productivity of the most productive journal X_1 can be written as:

$$X_1 = [A\Gamma(\rho + 1)]^{\frac{1}{\rho}} = (\rho - 1)^{-\frac{1}{\rho}} y_m^{\frac{\rho+1}{\rho}} \quad (6)$$

whereas the productivity of the r -th most productivity journal X_r is related to X_1 by $X_r = X_1 r^{-1/\rho}$. The comparison of the Gumbel's r -th characteristic extreme values with the mean of the simulation results are shown in Figure 2, from which it can be noted that though the Gumbel's

characteristic extreme theory can be used to predict the largest paper number X_1 , it cannot be used to estimate the other paper number in the core zone, X_r , $r = 2, 3, \dots, T_0$. Therefore, other methods must be used and it is assumed in this paper that all other X_r ($r = 2, 3, \dots, T_0$) are related to the largest paper number X_1 through the following equation:

$$\frac{X_1}{X_r} = k(r - 1) + 1 \quad (7)$$

where k is the only parameter waiting to be determined. This equation can be derived from the Equation (8) of Reference (Chen 1989), by assuming both $(r_i - r_1)/(r_1 + b)$ and $-1/c$ are relatively small. The validity of this equation can also be directly observed from Figure 2(b), where the blue circles denote the simulation results while the blue dashed lines denote the linear fitting results. Therefore, the productivity of the r -th most productive journals can be derived from Equation (7), and the accumulated productivity of the first r most productive journals can be written as:

$$R_c(r) = \sum_{i=1}^r \frac{X_1}{k(i - 1) + 1} \quad (8)$$

If there are T_0 journals with A_0 papers in the core region and the numbers of T_0 and A_0 are known, then the parameter k can be calculated from the equation $R_c(T_0) = A_0$. Then Equation (8) can be used to predict the evolution of the core regions ($r \leq T_0$) of the Bradford's curves.

2.2 Egghe's formula

After removing the T_0 journals and A_0 papers of the core region, the rest T_1 journals and A_1 papers match well with the theoretical results predicted by Equation (1), and therefore, they follow the Lotka's law and their Bradford curve can be predicted with the revised Leimkuhler and Egghe's formula, which can be written as (Egghe 1990):

$$R(r_1) = a \log(1 + br_1) \quad (9)$$

where the key parameters a and b are as follows:

$$a = \frac{A_1}{\log(e^\gamma y_m)} \quad (10)$$

$$b = \frac{e^\gamma y_m - 1}{T_1} \quad (11)$$

where γ is the Euler's number, $\gamma \approx 0.5772$, y_m is the journal productivity when the corresponding theoretical journal number $f(y_m) \approx 1$. y_m can be directly calculated from Equation (2), but can also be estimated from the following equation if all the values of X_1 , T_0 and A_0 are known:

$$y_m \approx \frac{X_1}{k(T_0 - 1) + 1} \quad (12)$$

Since the journal productivity of the core region is higher than the normal region, so the journal rank of these significant journals are lower than the normal ones. As a result, the Bradford curve of

the normal region will start at the point (T_0, A_0) and every ranking r_1 of the normal region should be transformed into $r = r_1 + T_0$, and the accumulated productivity of the first r journals $R(r)$ should be transformed into $R_n(r) = R(r_1) + A_0$. Then the revised Egghe's formula for the normal region can be written as:

$$R_n(r) = R(r - T_0) + A_0 = a \log[1 + b(r - T_0)] + A_0 \quad (13)$$

The revised Egghe's formula of Equation (13) can be used to predict the dynamic evolution of the normal regions ($T_0 < r < T$) of the Bradford's curve. Thus, it can be noted that Equations (8) and (13) can be used together to predict the dynamic evolution of the Bradford's curves.

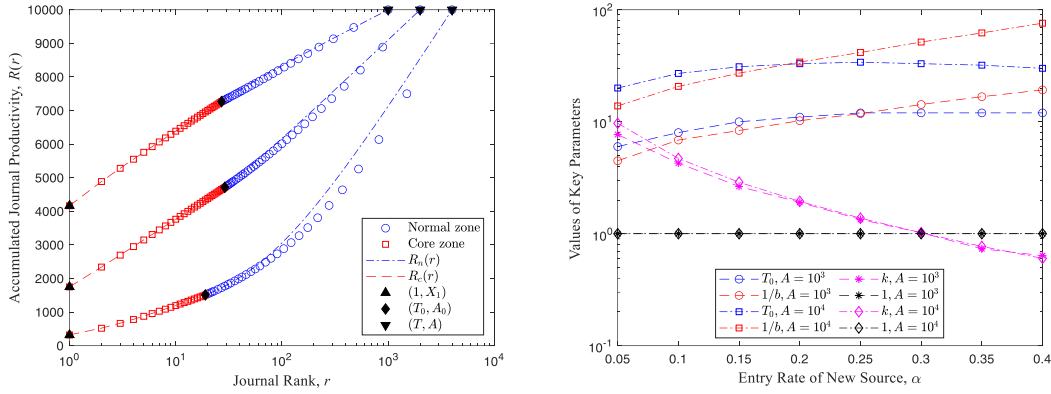


Figure 3 the cause of the Groos Droop and the Bradford's curve evolution. (a) the cause of the Groos Droop; (b) the evolution of Bradford's curve

The Bradford's curve is shown in Figure 3(b), from which it can be noted that the blue circles denote the normal zone, whereas the red squares denote the core zone. Meanwhile, the blue dashed lines denote the prediction results of Equation (13), whilst the red dotted lines denote the prediction results of Equation (8). The three black squares denote the $(1, X_1)$, the (T_0, A_0) and the (T, A) respectively. From the above discussion, it can be noted that the three points and two lines are most important parts for predicting the Bradford's curve evolution.

2.3 Groos Droop

The Groos is the first to note that when the productivity is low, then the curve with bend downward (Groos 1967). The cause of the Groos Droop has been explained by Egghe (Egghe and Rousseau 1988) as merging datasets, but it has been shown in this section that it is the existence of core region that causes the Groos Droop in the normal region.

The first and second derivatives of $R_c(r)$ of the core region can be derived from Equation (8):

$$\frac{\partial R_c(r)}{\partial(\log r)} = \frac{X_1 r}{k(r - 1) + 1} \quad (14)$$

$$\frac{\partial^2 R_c(r)}{\partial(\log r)^2} = \frac{X_1(1 - k)r}{[k(r - 1) + 1]^2} \quad (15)$$

From Equation (15), it can be noted that when $k > 1$, then $\frac{\partial^2 R_c(r)}{\partial(\log r)^2} < 0$ and the Bradford's

curve of the core region will concave downward, whereas when $k < 1$, then $\frac{\partial^2 R_c(r)}{\partial(\log r)^2} > 0$ and the Bradford's curve of the core region will concave upward. As the entry rate of new sources α increases, the journal number T will increase and the distributions of articles will become more dispersed. As a result, the largest journal productivity X_1 will decrease. Meanwhile, it can be noted from Equation (8) and $R_c(T_0) = A_0$ that lower X_1 indicates lower k if A_0 is relatively constant. Therefore, as α increases, the Bradford's curve of core region will gradually become concave upward, as shown by Figure 3.

Similarly, the first and second derivatives of $R_n(r)$ of the normal region can be derived from Equation (13):

$$\frac{\partial R_n(r)}{\partial(\log r)} = \frac{abr}{b(r - T_0) + 1} \quad (16)$$

$$\frac{\partial^2 R_n(r)}{\partial(\log r)^2} = \frac{ab(1 - bT_0)r}{[b(r - T_0) + 1]^2} \quad (17)$$

From Equation (17) it can be noted that when $T_0 > 1/b$ then $\frac{\partial^2 R_c(r)}{\partial(\log r)^2} < 0$, the Bradford's curve of the normal region will concave downward and thus show a Groos Droop, whereas when $T_0 < 1/b$ then $\frac{\partial^2 R_c(r)}{\partial(\log r)^2} > 0$, the Bradford's curve of the normal region will concave upwards and thus show a J-shaped curve. As the entry rate of new sources α increases, it can be noted from Figure 3(a) that the T_0 will gradually fall below $1/b$ and thus the Bradford's curve of the normal region will eventually become concave upward, which is similar to the case of the core region.

The variations of key parameters T_0 , $1/b$ and k with the entry rate α are shown in Figure 3 (b), from which it can be noted that when $A = 10^4$, the normal region will turn concave upward at critical point $\alpha_n \approx 0.2$ whilst the core region will turn concave upward at critical point $\alpha_c \approx 0.3$. Therefore, when $\alpha < 0.2$, the whole Bradford's curve will concave downward, and when $\alpha > 0.3$, the whole Bradford's curve will concave upward. When $0.2 < \alpha < 0.3$, the whole Bradford's curve will show a reversed S shape, with the core region concave downward and the normal region concave upward. The three shapes of Bradford's curves are shown in Figure 3 (a). In this particular case, since $\alpha_n < \alpha_c$, then there is no S-shaped Bradford's curve. This is because the aging of the sources are not considered here so the largest journal productivity X_1 is relatively large. When the effect of auto-correlation is considered, as discussed in Section 3, the corresponding X_1 will decrease significantly, which results in a lower k and thus a much lower α_c . When $\alpha_c < \alpha_n$, then the S-shaped Bradford's curve will appear if $\alpha_c < \alpha < \alpha_n$ with the core region concave upward and the normal region downward.

2.4 Bradford Dynamics

Since the analytical expression of T_0 , A_0 and X_1 (Equations (3), (4) and (6)) are all known, the core region of Bradford curve at any time can be predicted by using Equation (8). Since the key parameters of the normal regions can be derived from the above three factors through $T_1 = T - T_0$, $A_1 = A - A_0$ and Equation (12), the normal region of Bradford curve can be predicted by using Equation (13). From Figure 3 it can be noted that when $\alpha = 0.1$, then the whole

Bradford's will concave downward when $10^3 < A < 10^4$. The results shown in Figure are in accord with the theoretical prediction. The key parameters as functions of the journal paper number are shown in Figure 4(b), from which it can be noted that the theoretical results match with the numerical ones very well. It can also be noted that all these key factors are linear functions of the paper number A , therefore, Equation (18) will be used for studying the variations of T_0 , A_0 and X_1 for the more complicated scenarios.

$$\log(Y) = a_\rho + b_\rho \log(A) \quad (18)$$

where the constant a_ρ and b_ρ are functions of ρ . Since ρ is approximately one, then a_ρ and b_ρ can be viewed as constants.

The Bradford's curves of the constant entry rate scenario are shown in Figure 4(a), where the red squares and blue circles denote the simulation results of the core and normal regions respectively, whereas the red dashed lines and blue dotted lines denote the theoretical results of Equations (8) and (13) respectively. The three key points of $(1, X_1)$, (T_0, A_0) and (T, A) are also shown as black upper triangle, diamond and lower triangle respectively in Figure 4(a). From Figure 4(a) it can be noted that the although the core region includes far fewer journals than the normal region, its share of representation is significant due to the log scale of x-axis. Therefore, journals with lower ranks are better represented in Figure 4(a).

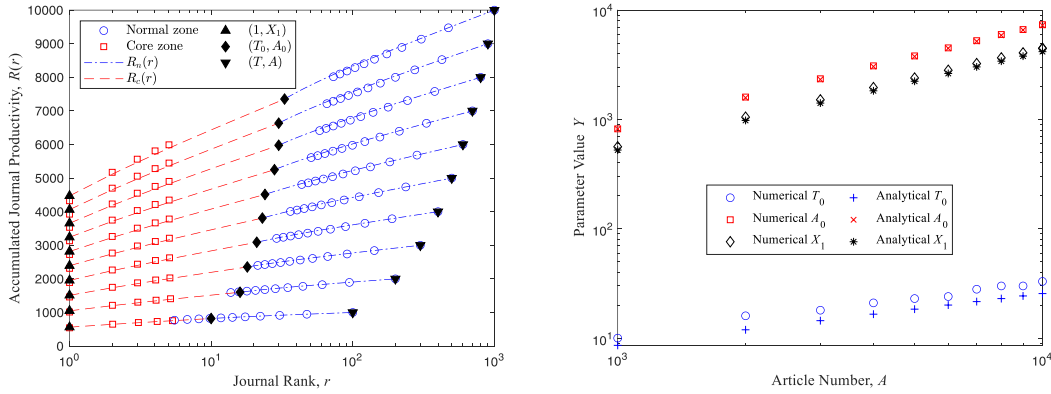


Figure 4 the dynamics of the Bradford's curve and the variation of the key parameters. (a) the dynamics of the Bradford's curves; (b) the variations of the key parameters

The simulation and analytical results of the T_0 , A_0 and X_1 are shown in Figure 4(b), where the hollow symbols denote the simulation results whereas the solid symbols denote the analytical ones. From Figure 4(b) it can be noted that the three key factors are all linear functions of the paper number A in the log-log axis, just as Equation (18) indicates. It is also notable that the analytical results match very well with the numerical ones, which verifies the validity of Equations (3), (4) and (6). The analytical result of T_0 is slightly lower than the numerical ones because the γ_m is higher than the numerical results.

3 Numerical Study

3.1 Decreasing Entry Rate

If we assume the probability of adding a new journal decreases linearly with the time.

$$\alpha(i) = \alpha_s - ki \quad (19)$$

where k is a constant, $k = (\alpha_s - \alpha_f)/A_f$, where α_f and A_f are the entry rate of new sources and the total article number in the final state respectively. Then the accumulated journal numbers can be written as:

$$T = \sum_{i=1}^A \alpha(i) = \alpha_s A - \frac{1}{2} k A^2 \quad (20)$$

According to Equation (20), quadratic fitting of T and A can be used to determine the value of α_s and α_f . After the α_s and α_f are determined, the $\bar{\alpha} = (\alpha_s + \alpha_f)/2$ can be used to calculate the analytical results.

The Bradford's curve and variations of key parameters are shown in Figure 5, from which it can be noted that the proposed method can still predict the variations of Bradford's curves well. In general, the analytical results of the $\bar{\alpha}$ matches well with the simulation results. The numerical results of A_0 and X_1 are slightly lower than the analytical ones. Therefore, the decreasing of entry rate has an additional negative effect on the increase of A_0 and X_1 .

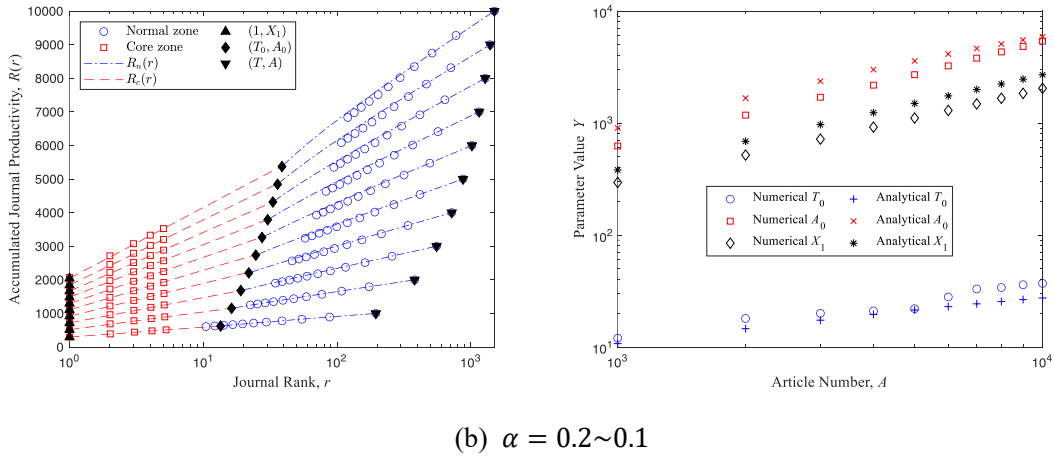
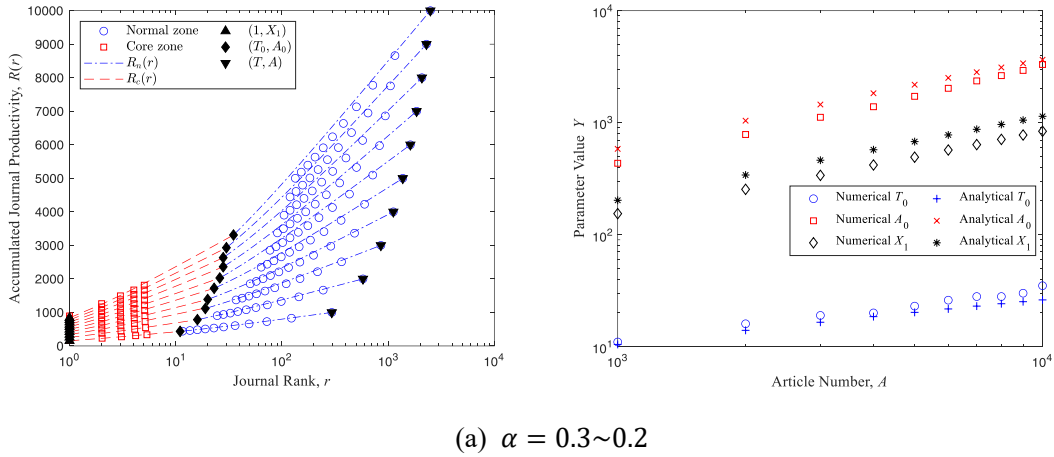


Figure 5 the dynamics of the Bradford's curve and the variation of the key parameters (a) when the entry rate decreases from 0.3 to 0.2; (b) when the entry rate decreases from 0.2 to 0.1.

From Figure 5, it can also be noted that the effect of decreasing entry rate on the shape of Bradford's curve and the variation of key factors are relatively insignificant. So, it is still possible to use the analytical results of constant entry rate $\bar{\alpha}$ for predicting the key parameters without introducing too much error.

3.2 Decaying Rate

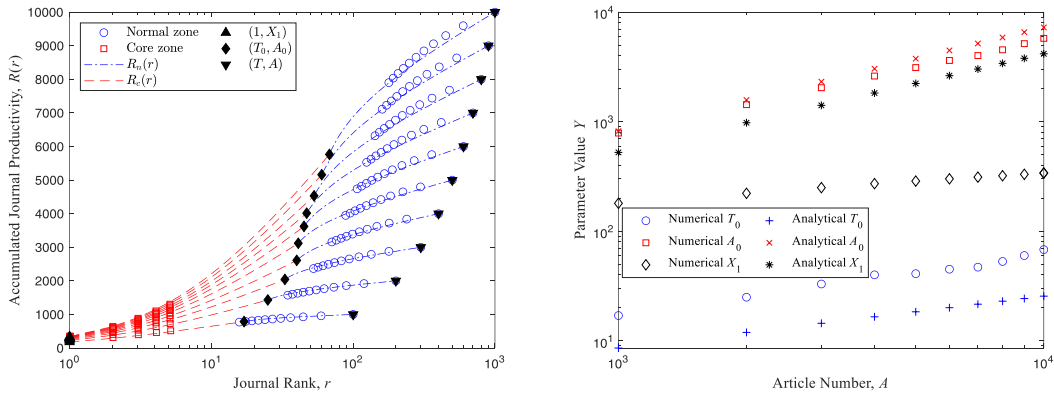
Simon's assumption is that only one paper gets published in each time period. He models the probability of a journal increasing in size in the next period as being proportional to a weighted sum of its past increments. These increments are weighted by a factor that decreases geometrically over time, with the rate of decrease denoted as γ .

Let $y_j(k)$ be the change in size of the j th journal during the k th time interval, where $y_j(k)$ is either unity or zero (the journal either experiences a unit increment in size or remains the same size during any given time interval). Then the size of the j th firm at the end of the k th interval is simply $\sum_{\tau=1}^k y_j(\tau)$. The expected increment in size of the j th firm during the $(k+1)$ th interval is:

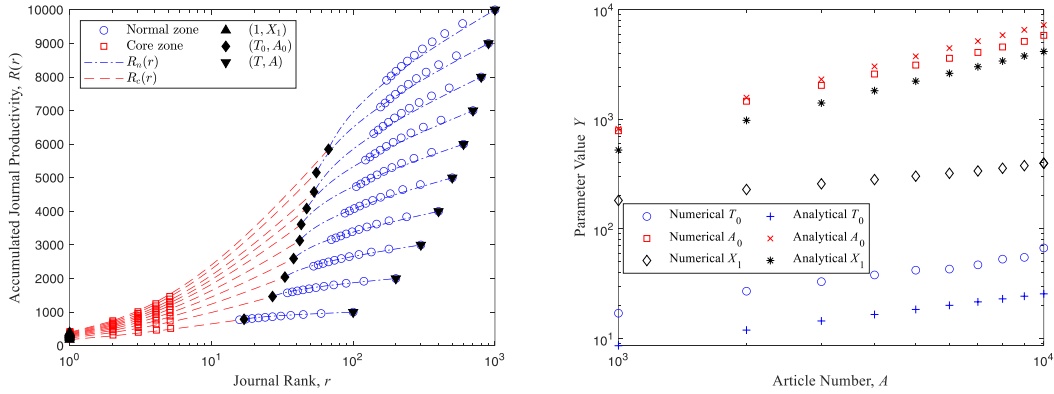
$$p[y_j(k+1) = 1] = \frac{1}{W_k} \sum_{\tau=1}^k y_j(\tau) \gamma^{k-\tau} \quad (21)$$

where W_k is a function of time that is the same for all journals, $W_k = \sum_{j=1}^T w_j(k)$, where $w_j(k) = \sum_{\tau=1}^k y_j(\tau) \gamma^{k-\tau}$, and γ is the fraction that determines how rapidly the influence of past growth on new growth dies out.

Figure 6 illustrates the impact of the decaying rate γ on the dynamics of Bradford's curves and the variations of key parameters. It's evident that the aging term notably increases T_0 , causing the normal region to become more concave downward. The aging term also markedly reduces X_1 by undermining the Mathew effect. As old article sources lose their appeal for new papers, the "success breeds success" effect diminishes, resulting in a significant decrease in X_1 , as depicted in Figure 6(a). Consequently, while the article number A_0 in the core zones remains relatively unchanged, T_0 needs to increase to compensate for the reduction of X_1 . This expansion of the core region enlarges its share of the Bradford's curve, tending to shape it into a J-shape due to the reduction of k and X_1 , as discussed in Section 2.3. Additionally, with the significant increase in T_0 , it's more likely that T_0 will exceed $1/b$, further contributing to the concave downward shape of the normal region. In summary, the decaying rate facilitates the Bradford's curve to adopt an S-shaped form more easily.



(a) $\alpha = 0.1, \gamma = 0.95$



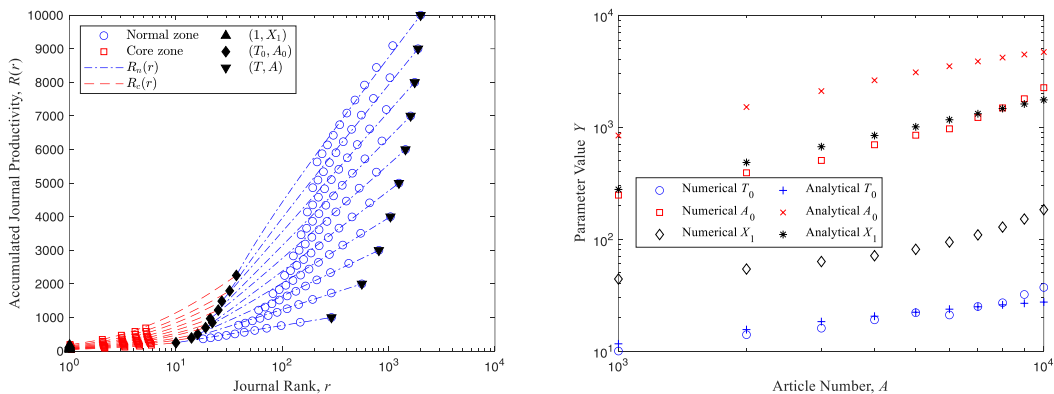
(b) $\alpha = 0.1, \gamma = 0.95 \sim 1.0$

Figure 6 the dynamics of the Bradford's curve and the variation of the key parameters. (a) when the entry rate is 0.1 and the decaying rate is 0.95; (b) when the entry rate is 0.1 and the decaying rate increases from 0.95 to 1.0

3.3 Varying Decaying and Entry Rate

Figure 7 illustrates the impact of changing decaying and entry rates on Bradford's curve. In real-world scenarios, both the entry rate of new sources and the decaying rate often fluctuate. For instance, the entry rate might linearly shift from 0.3 to 0.1, while the decaying rate linearly shifts from 0.95 to 1.0. Observing Figure 7, it becomes apparent that increasing the decaying rate and decreasing the entry rate generally exert opposite effects on Bradford's curve.

When the entry rate α decreases and the decaying rate γ varies or remains constant, the largest journal productivity X_1 also diminishes due to reduced Mathew effect. Consequently, the core region is likely to exhibit a J-shaped curve, resembling scenarios with constant α and varying or constant γ . However, the total article number A_0 in the core region significantly deviates from analytical results, while the total journal number T_0 in the core region remains relatively consistent with analytical predictions—similar to scenarios involving decreasing α and opposite to scenarios with γ . As a result, the normal region of Bradford's curve becomes less concave downward, with its starting point on the y-axis notably lower, resembling trends seen with decreasing entry rates rather than decaying rates. Notably, all three key factors continue to exhibit linear relationships with article number, suggesting Equation (18) remains viable for predicting them.



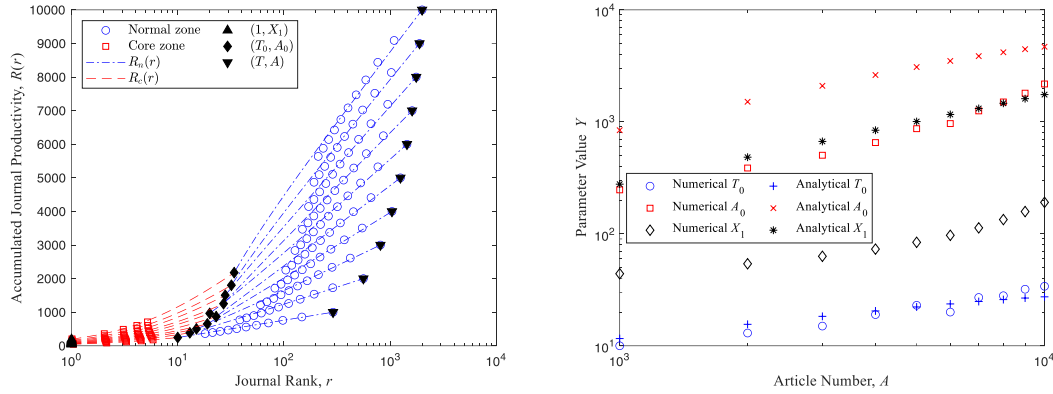
(a) $\alpha = 0.3 \sim 0.1, \gamma = 0.95$ (b) $\alpha = 0.3 \sim 0.1, \gamma = 0.95 \sim 1.0$

Figure 7 the dynamics of the Bradford's curve and the variation of the key parameters. (a) when the entry rate decreases from 0.3 to 0.1 and the decaying rate is 0.95; (b) when the entry rate decreases from 0.3 to 0.1 and the decaying rate increases from 0.95 to 1.0.

4 Empirical Study

4.1 Dataset of Croatian Chemistry Research

The research output in chemistry of authors from Croatia was used by Oluić-Vuković for the preparation of full bibliographic references for a ten-year period (Oluić-Vuković 1992). Only articles published in journals were taken into consideration and the dataset comprises 2543 papers published in 416 journals over a 10-year interval. The journal productivity of the first few (less than 10) most productive journals was directly taken from Figure 1 of Reference (Oluić-Vuković 1992) whilst the productivity of the other journals was directly taken from Tables 4 and 6 of Reference (Oluić-Vuković 1998). Data taken from the figures were adjusted to comply with the total number of journals and articles obtained from the Table 2 of Reference (Oluić-Vuković 1992).

In order to predict the dynamics of the Bradford's curve, the first step is to predict the variation of total article number $A(t)$ with time t . Logistic regression analysis (Verhulst 1838) is applied to the empirical data so that the total article number $A(t)$ at any time can be predicted, as shown in Figure 8(a). After that, the total journal number T and the entry rate of new sources α can be estimated by plotting the total journal number T against the total article number A and applying the linear fitting of $T = A\alpha$, as shown in Figure 8(b). After the point (T, A) is determined for any time, then linear regression of Equation (18) is employed to determine the three key parameters of T_0 , A_0 and X_1 in the log-log axis, and the fitting results are shown in Figure 9(a). Then the key points of (T_0, A_0) and $(1, X_1)$ at any time can be determined. Finally, based on the three key points, Equations (8) and (13) can be used to determine the Bradford curve for the core region and the normal region respectively, and the results are shown as the red dashed lines and blue dotted lines in Figure 9(b) respectively.

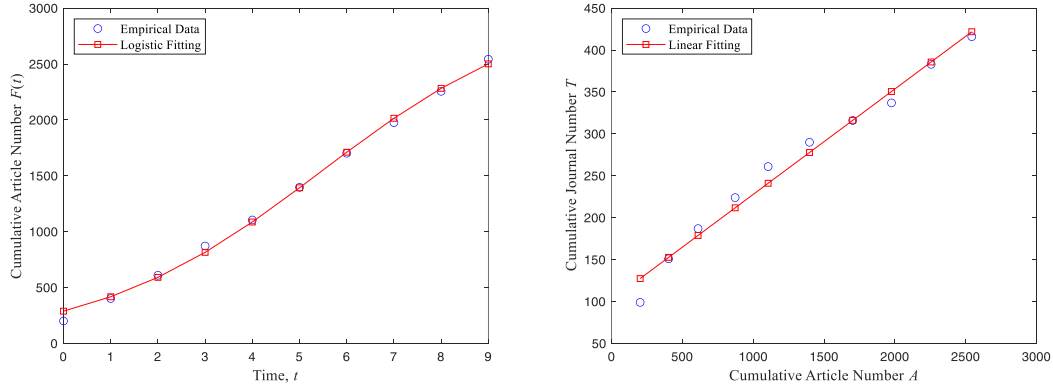


Figure 8 the dynamics of the Bradford's curve and the variation of the key parameters. (a) the dynamics of the Bradford's curves; (b) the variations of the key parameters

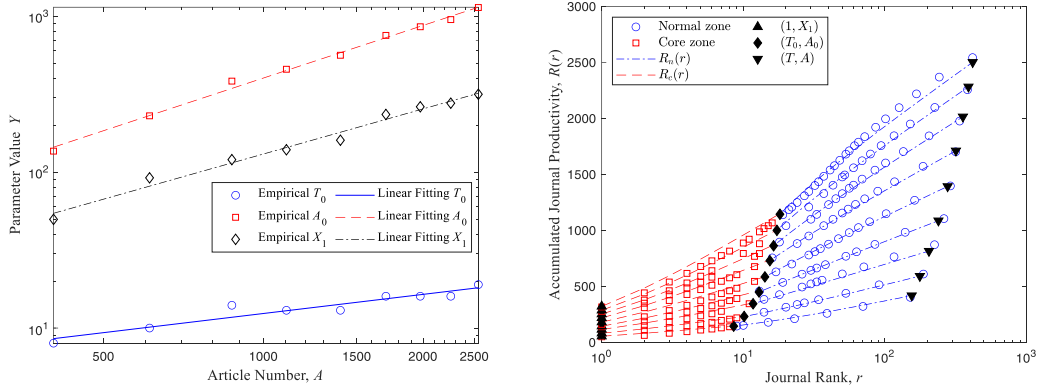


Figure 9 the dynamics of the Bradford's curve and the variation of the key parameters. (a) the dynamics of the Bradford's curves; (b) the variations of the key parameters

From Figure 9(b) it can be noted that the Bradford's curve gradually turns from J-shape into S-shape, and this transition is well captured by the analytical prediction.

4.2 Dataset of Solar Power Research

The bibliographies on solar power research for the year 1971, 1974, 1977, 1980, 1983 and 1986 for the paper published in journals from Engineering Index were prepared by Garg et al. (Garg, Sharma et al. 1993). The data used in the following analysis are directly taken from the Tables 1~7 of Reference (Garg, Sharma et al. 1993).

Similar to the case of the Croatia Chemistry Dataset, the prediction of the dynamics of the Bradford's curve also includes the following four steps:

1. Applying the logistic regression fitting to the empirical data of cumulative article number vs time (obtained From Table 7) to obtain the prediction of article number of the desired intervals, as shown in Figure 10(a).
2. Applying the quadratic fitting of Equation (20) to the journal and article pairs to obtain the estimated journal number T and entry rate of new sources α at any article number A , as shown in Figure 10(b).

3. Applying the linear fitting of Equation (18) to the empirical data of T_0 , A_0 and X_1 in the log-log axis to obtain their predictions at any article number A , as shown in Figure 11(a).
4. Applying the Equations (8) and (13) to draw the Bradford's curve of the core region and normal region respectively, as shown in Figure 11(b).

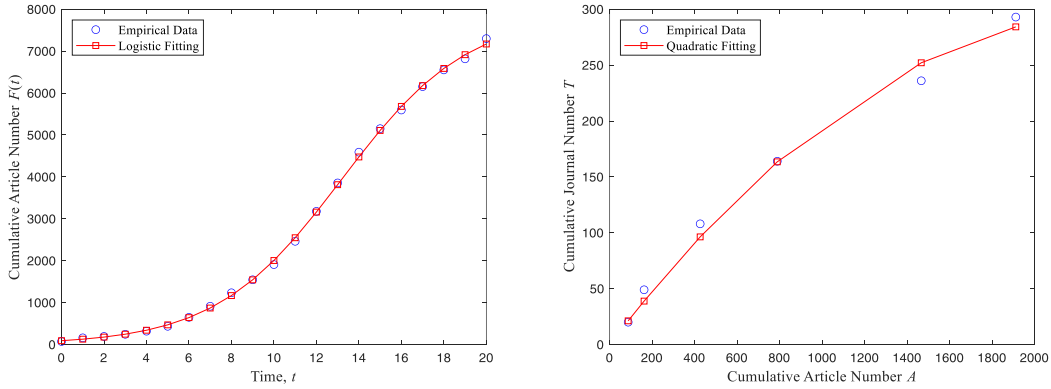


Figure 10 the dynamics of the Bradford's curve and the variation of the key parameters. (a) the dynamics of the Bradford's curves; (b) the variations of the key parameters

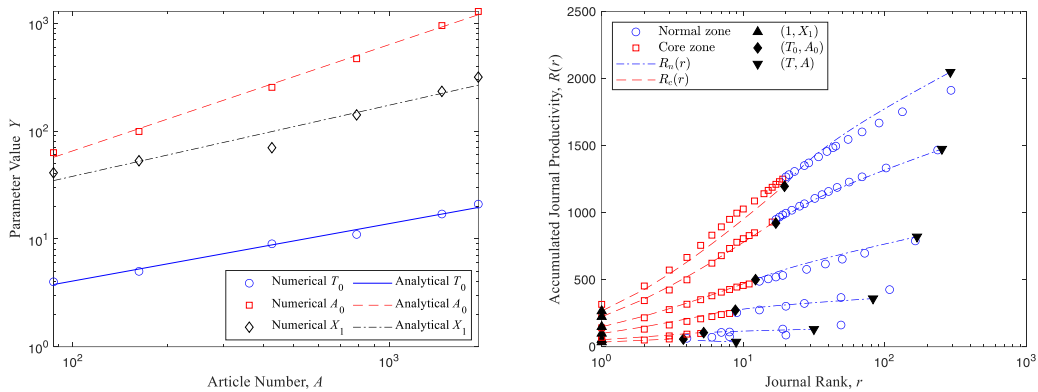


Figure 11 the dynamics of the Bradford's curve and the variation of the key parameters. (a) the dynamics of the Bradford's curves; (b) the variations of the key parameters

From Figures 9(b) and 11(b) it can be noted that though our suggested method can roughly predict how Bradford's curves change over time, there are still some errors present. This is because Bradford's law inherently contains uncertainties or errors. Our numerical analysis shows that the number of articles for each journal rank has a large standard deviation, making it practically impossible to precisely predict the shape of Bradford's curve. Additionally, our method involves several fitting procedures, introducing errors in the process. Thus, while our approach can give a general idea of how Bradford's dynamics might unfold, it cannot accurately forecast the number of articles for each journal at any given time.

Another issue with our method is that the first derivatives of the core region (Equation (14)) and the normal region (Equation (16)) differ at the point (T_0, A_0) . This leads to the analytical curve being jagged at the intersection point, whereas the numerical simulation results show smoothness throughout. One potential solution to this problem is to propose a more complex formula for the normal region, but this would inevitably complicate the entire method. Given the

difficulty in precisely predicting Bradford's curve dynamics, this aspect is not explored further in our research.

5 Conclusion

In this paper, we delve into how integer constraints, specifically the limits imposed by the number of journals T and articles A , affect the shape of Bradford's curve. We categorize Bradford's curve into two zones: the core zone and the normal zone, based on whether the integer effect plays a significant role. Utilizing the Simon-Yule model, we derive analytical results for key parameters and distributions under constant entry rate conditions. Then, we formulate theoretical equations for each zone and analyze the reasons behind the diverse shapes of Bradford's curves. Monte Carlo simulations help us explore how decreasing entry rates of new sources and decay rates impact the curve's shape and key parameters. Finally, we validate our approach using empirical data from Croatian Chemistry and Solar Power datasets, demonstrating its ability to predict Bradford's curve dynamics. From our findings, we draw several conclusions:

1. Bradford's curve should be divided into distinct zones based on the significance of integer constraints, each requiring separate formulae.
2. The shape of Bradford's curve can take on four different forms, determined by the second derivatives of the core and normal zones.
3. Key parameters such as the maximum productivity X_1 , journal number T_0 , and article number A_0 play crucial roles in shaping Bradford's curves, with entry rate and decay rate changes influencing these parameters.
4. Despite some errors, our proposed four-step method can effectively predict general trends in Bradford's curves.

These insights can guide academic libraries in procuring and utilizing scientific literature effectively.

6. Statements and Declarations:

Funding and Conflicts of interests: The research leading to these results received funding from the Library Society Guangdong under Grant Agreement No. GDTK23004. This article is one of the achievements of the 2023 Key Research Project of Guangdong Provincial Library titled "Joint Analysis and Data Governance of Papers and Patents in the Context of Smart Libraries" (Project Number: GDTK23004).

7 References

Barrantes, B. S. L., S. Dalton and D. Andre (2023). "Bibliometrics methods in detecting citations to questionable journals." *The Journal of Academic Librarianship* **49**(4): 102749.

Bradford, S. C. (1934). "Sources of information on specific subjects." *Engineering* **137**: 85-86.

Chen, Y.-S. (1989). "Analysis of Lotka's law: the Simon-Yule approach." *Information Processing & Management* **25**(5): 527-544.

Chen, Y.-S., P. P. Chong and M. Y. Tong (1994). "The Simon-Yule approach to bibliometric modeling."

Information Processing & Management **30**(4): 535-556.

Chen, Y.-S. and F. F. Leimkuhler (1987). "Bradford's law: An index approach." Scientometrics **11**: 183-198.

Chen, Y. S., P. P. Chong and M. Y. Tong (1995). "Dynamic behavior of Bradford's law." Journal of the American Society for Information Science **46**(5): 370-383.

Egghe, L. (1985). "Consequences of Lotka's Law for the Law of Bradford." Journal of Documentation **41**(3): 173-189.

Egghe, L. (1990). "Applications of the theory of Bradford's law to the calculation of Leimkuhler's law and to the completion of bibliographies." Journal of the American Society for information Science **41**(7): 469-492.

Egghe, L. and R. Rousseau (1988). "Reflections on a deflection: a note on different causes of the Groos droop." Scientometrics **14**(5-6): 493-511.

Garg, K., P. Sharma and L. Sharma (1993). "Bradford's law in relation to the evolution of a field. A case study of solar power research." Scientometrics **27**(2): 145-156.

Glänzel, W. (2010). "The role of the h-index and the characteristic scores and scales in testing the tail properties of scientometric distributions." Scientometrics **83**(3): 697-709.

Glänzel, W. (2013). "High-end performance or outlier? Evaluating the tail of scientometric distributions." Scientometrics **97**(1): 13-23.

Groos, O. V. (1967). "Brief Communications Bradford's Law and the Keenan-Atherton Data." American Documentation (pre-1986) **18**(1): 46.

Ijiri, Y. and H. A. Simon (1977). Skew distributions and the sizes of business firms, North-Holland.

Larivière, V., É. Archambault and Y. Gingras (2008). "Long-term variations in the aging of scientific literature: From exponential growth to steady-state science (1900–2004)." Journal of the American Society for Information Science and technology **59**(2): 288-296.

Leimkuhler, F. F. (1967). "The Bradford distribution." Journal of documentation **23**(3): 197-207.

Oluić-Vuković, V. (1989). "Impact of productivity increase on the distribution pattern of journals." Scientometrics **17**(1-2): 97-109.

Oluić-Vuković, V. (1991). "The shape of the distribution curve: An indication of changes in the journal productivity distribution pattern." Journal of Information Science **17**(5): 281-290.

Oluić-Vuković, V. (1992). "Journal productivity distribution: Quantitative study of dynamic behavior." Journal of the American Society for Information Science **43**(6): 412-421.

Oluić-Vuković, V. (1997). "Bradford's distribution: From the classical bibliometric "law" to the more general stochastic models." Journal of the American Society for Information Science **48**(9): 833-842.

Oluić-Vuković, V. (1998). "Simon's generating mechanism: Consequences and their correspondence to empirical facts." Journal of the American Society for Information Science **49**(10): 867-880.

Qiu, L. and J. Tague (1990). "Complete or incomplete data sets. The Groos droop investigated." Scientometrics **19**: 223-237.

Sen, S. and S. Chatterjee (1998). "Bibliographic scattering and time: an empirical study through temporal partitioning of bibliographies." Scientometrics **41**(1-2): 135-154.

Sheikh, A., A. Q. Zahra and J. Richardson (2022). "Scholarly open access journals in medicine: A bibliometric study of DOAJ." The Journal of Academic Librarianship **48**(3): 102516.

Simon, H. A. (1955). "On a class of skew distribution functions." Biometrika **42**(3/4): 425-440.

Simon, H. A. and T. A. Van Wormer (1963). "Some Monte Carlo estimates of the Yule distribution." Behavioral Science **8**(3): 203-210.

Verhulst, P. (1838). "Notice on the law that the population follows in its growth." Corresp Math Phys **10**: 113-126.

Vickery, B. C. (1948). "Bradford's law of scattering." Journal of documentation **4**(3): 198-203.

Wagner-Döbler, R. (1997). "Time dependencies of Bradford distributions: Structures of journal output in 20th-century logic and 19th-century mathematics." Scientometrics **39**: 231-252.